

The use of textural features on the polarimetric SAR image classification*

SIDNEI JOÃO SIQUEIRA SANT'ANNA
CORINA DA COSTA FREITAS
CAMILO DALELES RENNÓ

INPE--Instituto Nacional de Pesquisas Espaciais
Caixa Postal 515, 12201- 097 São José dos Campos, SP, Brazil
{sidnei,corina,camilo}@dpi.inpe.br

Abstract. In this work the potentiality of the textural information that polarimetric SIR-C data can provide to discriminate some types of land use is studied. That information is extracted from the data by using statistical and distributional measures. The Euclidean distance is used to select the best set of features for discriminating classes of interest. Features bands (textural bands) are built by filtering the images, and they are used as channels on ICM classification. The discriminatory power of the selected features is assessed by analyzing the classification results, which are evaluated using the confusion matrix and the Kappa coefficient of agreement. The results show that the textural information, as well as the tonal information provided by these images are very important to discriminate the land use under study.

Keywords: feature extraction, textural attributes, polarimetric SAR data, classification.

1 Introduction

The Brazilian Amazonian Tropical Forest has been the object of several studies, particularly concerning the estimation of the extent and rate of gross deforestation. With an area of about 5 million square kilometers, 4 million of which covered by forest, a total of 517,069 square kilometers were deforested by 1996 (INPE, 1998). The knowledge and understanding of tropical deforestation process and its consequences are important aspects of global change, and they are necessary for the Brazilian Government to take actions for the sustainable use of the natural resources.

Besides the importance of mapping the deforested areas, the study of secondary succession is also important due to the impact that these areas have on the region carbon cycle balance, which might have consequences on the global climate change and on the carbon budget. Compared to primary formations, the secondary forest accumulate biomass more rapidly and therefore act as a net sink for atmospheric carbon (Brown and Lugo, 1990), but this net sink is still poorly quantified (Schimel, et al., 1995).

* This work was supported by grants from PPG-7 (0808/95 and 0816/95), Convênio FINEP (6.6.96.0473.00 and 6.6.96.0474.00).

Many studies that have been done in Brazilian Amazonian still use LANDSAT-TM data to map and to monitor the changes in forests, deforested areas and regenerating forests. However, weather conditions strongly limit the data availability. The use of radar data is therefore the only way of overcoming this problem. In addition to the all weather capability of radar and the availability of currently systems (ERS, JERS, RADARSAT, airborne systems, etc), the use of radar data to monitor deforestation and regeneration is strongly motivated by the sensitivity of the radar backscatter to standing biomass (Le Toan et al., 1992; Ranson et al., 1995; Luckman et al., 1997b; Yanasse et al., 1997).

The number of studies in Amazon using radar data has increased for those reasons. Nevertheless, proper methods for extracting information from radar images are still object of study, and they are dependent of the type of application (estimation of above ground biomass, mapping of deforested areas, identification of different kind of crops, classification of specific land use, among others) and the sensor characteristics, as polarization (HH, HV, VH and VV), band (C, L, X, Ku, P, etc), angle of illumination, pixel resolution, etc.

The extraction of the information from images is usually derived from tonal analysis. However, only tonal information is not sufficient to gather all information provided by SAR images. Therefore, many researchers have used textural attributes to extract the complementary information (see, for instance, Luckman et al., 1997a; Sant'Anna et al., 1997; Soares, et al., 1997).

The objective of this paper is to analyze and to select several texture features (attributes) from radar images, for the discrimination of some land use classes (primary forest, different stages of secondary forest, bare soil and pasture). After a brief description in **Section 2** about the study area and the data used, the methodology is detailed in **Section 3**, pointing out the whole process of extraction and selection of features used for land cover classification. The results are presented in **Section 4**, and **Section 5** was reserved for the final conclusions of the work.

2 Study area and data

The study area is located on Pará State, Brazil, in the Tapajós National Forest. Although this Forest is a reserved area, in the study site there are primary forest and deforested regions. Some deforested regions were abandoned and are presently under regeneration. Besides the importance of mapping these regions, another reason for choosing the Tapajós area is the availability of different remote sensing data and field work information. Among these data set, a multi-temporal LANDSAT/TM images from 1984 to 1995 (except 1994) are available, which were used to build a regeneration stage map of the area, as described in details in Sant'Anna et al.(1995).

Several radar data are also available for this area, such as JERS-1 (L-HH band polarization), RADARSAT (C-HH band polarization), SAREX (C-HH and C-VV band polarization), ERS-1 (C-VV band polarization), and SIR-C (L and C bands, HH and HV polarization). To reach the objectives of this work, the SIR-C data were chosen, because they have higher discrimination potentiality than the other radar sensors due to the possibility of combining different bands and polarization. The SIR-C images used in this paper are part (950 columns by 1400 lines) of the images obtained on October 1994, with approximately 8 nominal looks.

A color composite of the SIR-C images is shown in **Figure 1a**, with L-HH, L-HV and C-HH in the red, green and blue channels, respectively. In **Figure 1b** is depicted the regeneration stage map, where the classes are represented by colors as following: primary forest (Forest) in dark green, old regeneration (OldReg – secondary succession with more than or equal to 8 years old) in light green, new regeneration (NewReg – secondary succession with less than 8 years old) in yellow, recent activities (RecAct - bare soil, pasture and some agricultural crops) in magenta, clouds and shadows in black and regions without information in gray. The light and dark blue areas appearing on **Figure 1a** refer to deforested areas. There are not many areas of the OldReg class, and it is very difficult to see them on **Figure 1a** because they have a very similar pattern than those presented by the Forest class (reddish tone). In fact, the visual confusion between these two classes is apparently bigger than the confusion among others classes. Some most representative areas of the OldReg class are indicated by white arrows in **Figure 1b**.

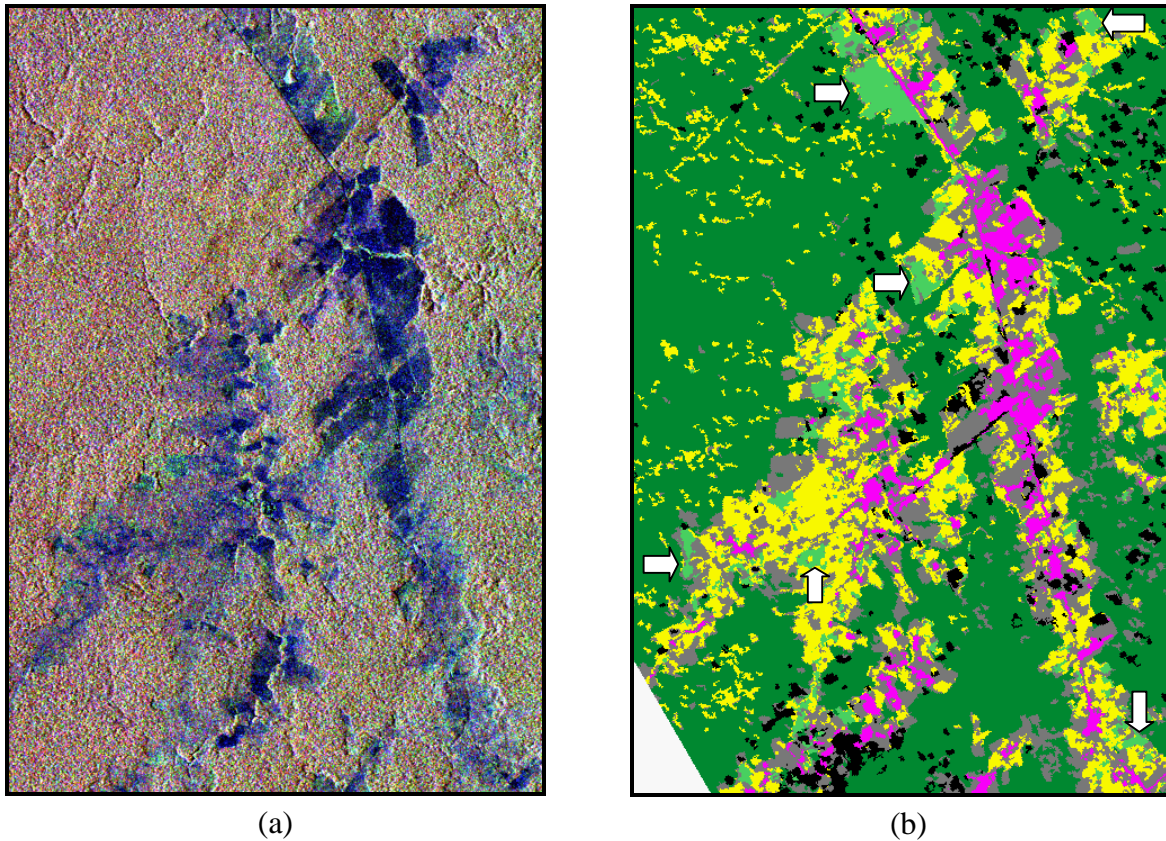


Figure 1: Study area: (a) SIR-C color composite L-HV(R), L-HH(G) and C-HH(B) and (b) Regeneration stage map.

3 Methodology

The regeneration map was used as a mask over SIR-C images, after registering the map to these images. In this registration process the SAR images were the base images and the map was the wrapping image, in order to not modify the SAR data properties. After the map had been registered, its regions (classes) could be associated with SAR data. To avoid errors such as

register displacements and precise identification of the classes boundaries, a morphological operator, called erosion, was applied to the map using a 3x3 window.

The analysis was followed by features extraction. Two kind of measures denominated statistical (including first and second order statistical measures) and distributional (including parameters that characterize statistical distributions) were used as features. The former were computed in amplitude and intensity data and they are represented with subscript A and I, respectively, while the latter were computed only in amplitude data.

The statistical measures were defined by: mean (μ_A and μ_I), mean in dB (μ_{dB}), standard deviation (σ_A and σ_I), coefficient of variation (CV_A), autocorrelation for lags (0,1), (1,0) and (1,1), represented by $\rho_A(0,1)$, $\rho_A(1,0)$ and $\rho_A(1,1)$, respectively, and coefficient of variation for the same lags, represented by $CV_A(0,1)$, $CV_A(1,0)$ and $CV_A(1,1)$. The definition of the coefficient of variation for lag (s_x, s_y) is given by:

$$CV_A(s_x, s_y) = \frac{\sqrt{\hat{g}(s_x, s_y)}}{m_A}$$

where $\hat{g}(s_x, s_y)$ is the estimated autocovariance for lag (s_x, s_y) , with s_x and s_y representing the distances between pixels in the two orthogonal directions x and y .

The distributional measures are estimated parameters from distributions that are widely used on SAR data modeling. The selection of the distributions was based on a χ^2 -goodness-of-fit test for the Gaussian (N), Log-Normal (LN), Weibull (W), Square Root of Gamma ($\Gamma^{1/2}$), K-Amplitude (K_A) and G0-Amplitude (G_A^0) distributions. Before doing the goodness-of-fit test the data were sub-sampled in a 1 to 4 ratio (only one pixel every 2x2 window was used), to reduce the effect of spatial correlation on test statistics. The LN , $\Gamma^{1/2}$, K_A and G_A^0 were the best distributions fitted to sample data and their parameters were chosen as discriminant measures, except the parameter for the $\Gamma^{1/2}$ which is related to the mean value of the data, and it is already considered into the statistical measures. Therefore, the parameters used in the analysis were: mean and standard deviation of the LN distribution (m_{LN} and s_{LN}), and the α parameter of the K_A and G_A^0 distributions (a_{KA} and a_{GA0}). For details about these distributions and their parameters' estimators, the reader is referred to Vieira (1996) and Frery et al. (1997a).

The estimators of the parameters for the K_A and G_A^0 distributions involve the equivalent number of looks (N). The equivalent number of looks for SIR-C images was estimated from intensity data, using $\hat{N} = 1/CV^2$ for samples from homogeneous areas (recent activities class for C bands and old regeneration class for L bands). The estimated values of \hat{N} for each pair of band/polarization and their mean are shown in **Table 1**. The mean value was used on the estimation of the a_{KA} and a_{GA0} parameters for all pair of band/polarization.

TABLE 1 - Estimated number of looks and overall mean, for SIR-C images.

Band/Polarization	C-HH	C-HV	L-HH	L-HV	Overall Mean
\hat{N}	6.06806	6.28219	6.10203	5.33963	5.94798

The estimation of the sixteen measures (12 statistical and 4 distributional) was conducted for each class in the four original bands (with a total of sixty-four features), considering only regions which had the number of pixels greater than or equal to 100. **Table 2** gives the number of regions and the total number of pixels before and after sub-sampling. The sub-sampling was used only for the goodness-of-fit test. Parameters estimation was performed using the whole data sets to obtain more accurate values.

TABLE 2 - Number of regions and pixels used on the measures estimation.

Classes	Regions	Pixels (after Sub-sampling)
RecAct	75	47,689 (8,535)
NewReg	358	177,753 (27,894)
OldReg	114	55,923 (9,975)
Forest	70	2,217,098 (433,076)

The selection of the features with the highest discriminatory power for the classes of interest was based on the Euclidean distance for each pair of classes (RecAct-NewReg, RecAct-OldReg, RecAct-Forest, NewReg-OldReg, NewReg-Forest, and OldReg-Forest). All estimated features were standardized by taking the values and dividing them by its maximum value, so they would range from 0 to 1. The influence of outliers on the estimated features was minimized by trimming them on 10%. After the selection of the “best” discriminatory attributes, bands of these attributes were generated by a filtering process.

These bands of attributes and the original images were used to perform several classifications. The Gaussian Multivariate Maximum Likelihood (ML) and the Multivariate Iterated Conditional Modes (ICM) were used as classifiers (Frery et al., 1997b and Vieira et al. 1997). The images resulting from the ML classification were used as one of the input for ICM classifier, which needs a contextual image to start the classification. The training and test samples were obtained from areas that had more than 250 pixels in the eroded regeneration stage map. The number of pixels utilized on both samples are presented in **Table 3**. In order to evaluate the classifications results, the confusion matrix and the Kappa coefficient of agreement were computed from the test samples. To verify the difference between two Kappa values a Z test was performed (Ma and Redmond, 1995).

TABLE 3 – Number of pixels for training and test samples.

Classes	Training	Test
RecAct	15,561	6,614
NewReg	58,315	28,553
OldReg	13,880	3,501
Forest	465,294	173,193

4 Results and Discussion

The Euclidean distance was computed for the trimmed and non-trimmed samples resulting in the same selected attributes. Therefore the analysis that follows is based on the non-trimmed samples. According to the analysis of Euclidean distance five attributes were selected to discriminate the six pairs of classes (**Table 4**). From the selected features it can be noted that only two bands (L-HH and L-HV) and four measures (m_{LN} , m_A , a_{KA} and m_l) were chosen. The C bands do not seem to carry any information with the measures used here to discriminate the classes under study, and L-HV band is the most important band for this purpose.

TABLE 4 – Selected features for discriminating pair of classes.

Pair of Classes	Selected Features
RecAct-NewReg	$m_{LN}(lhv)$
RecAct-OldReg	$m_{LN}(lhv)$
RecAct-Forest	$m_A(lhv)$
NewReg-OldReg	$a_{KA}(lhh)$
NewReg-Forest	$m_l(lhv)$
OldReg-Forest	$a_{KA}(lhv)$

The filtered images with these measures were built using windows of size 7x7 pixels, except for the α parameter of K-Amplitude that a window size of 11x11 pixels was used. However, when building the filtered image with $a_{KA}(lhh)$ parameter, the estimation of this parameter presented problems and therefore this attribute was changed to $CV_A(lhh)$. This CV_A measure was chosen, since it is highly correlated with a_{KA} and both measures seem to carry the same information (see Sant'Anna et al., 1997).

Five sets of images were generated and the ML/ICM classifications were performed for each set. These sets were:

- **Sirc2**: includes two original bands (L-HH and L-HV);
- **Sirc4**: includes the four original bands (C-HH, C-HV, L-HH and L-HV);
- **Sirc5**: includes the five bands generated by the selected attributes;
- **Sirc7**: includes the L-HH and L-HV original bands and the five attribute bands; and
- **Sirc9**: includes the four original bands and the five attribute bands.

The Sirc2 set includes only the L-HH and L-HV bands because they are the two bands appearing on the list of the five best selected features. These five sets were generated aiming at the comparison of the influence of the original and attribute bands on the classification results.

The ICM classifications for the sets described above are presented in **Figures 2 to 6**. In these figures the classes of RectAct, NewReg, OldReg and Forest are represented by magenta, yellow, light and dark green colors, respectively. The ML classification results are not presented here

since the ML classification was used as one of the inputs of ICM classifier and the results of the latter is usually much better than those obtained with ML classifier.

The evaluation of the classifications was assessed from confusion matrices and the Kappa coefficients of agreement and their sample variances (\hat{K} and \hat{S}_K^2), which are given in **Tables 5** to **9**, for the aforementioned classifications.

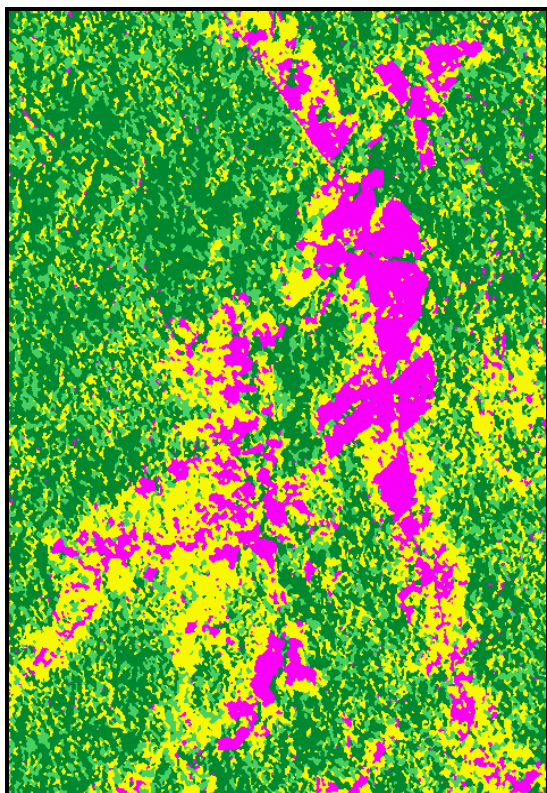


Figure 2: ICM classifications using Sirc2 set.

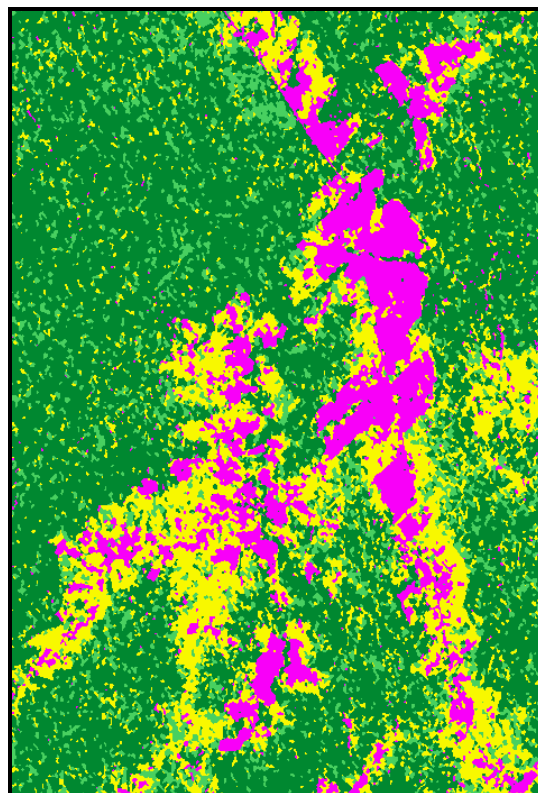


Figure 3: ICM classifications using Sirc4 set.

TABLE 5 – Confusion matrix for the Sirc2 set classification.

Classes\ Classif	RecAct	NewReg	OldReg	Forest
RecAct	91.0	7.6	0.2	1.2
NewReg	12.6	62.9	11.9	12.6
OldReg	8.6	52.3	25.4	13.7
Forest	1.3	22.0	20.7	56.0
$\hat{K} = 0.2515$		$\hat{S}_K^2 = 1.4016 \times 10^{-5}$		

TABLE 6 – Confusion matrix for the Sirc4 set classification.

Classes\ Classif	RecAct	NewReg	OldReg	Forest
RecAct	90.5	8.2	0.1	1.2
NewReg	12.3	64.6	13.5	9.6
OldReg	8.1	50.1	36.5	5.3
Forest	1.1	9.7	12.3	76.9
$\hat{K} = 0.4404$		$\hat{S}_K^2 = 1.7398 \times 10^{-5}$		

From the classification of the Sirc2 and Sirc4 sets (**Figures 2** and **3**) and from **Tables 5** and **6** it can be noticed that the Forest class is better classified when all the original bands (C-HH, C-HV, L-HH and L-HV) are used, instead when only the L bands are used. The confusion between

the Forest class and regeneration classes is greater on the Sirc2 set than the Sirc4 set. The addition of C bands improves the classification of Forest and OldReg classes, by decreasing the misclassification of Forest pixels as belonging to the regeneration classes, as well as the misclassification of OldReg pixels as belonging to the Forest class. The RecAct and NewReg classes do not suffered many changes on their classification results by including C bands in the Sirc2 set. These facts evidence the influence of the C bands on the discrimination between Forest class and regeneration classes.

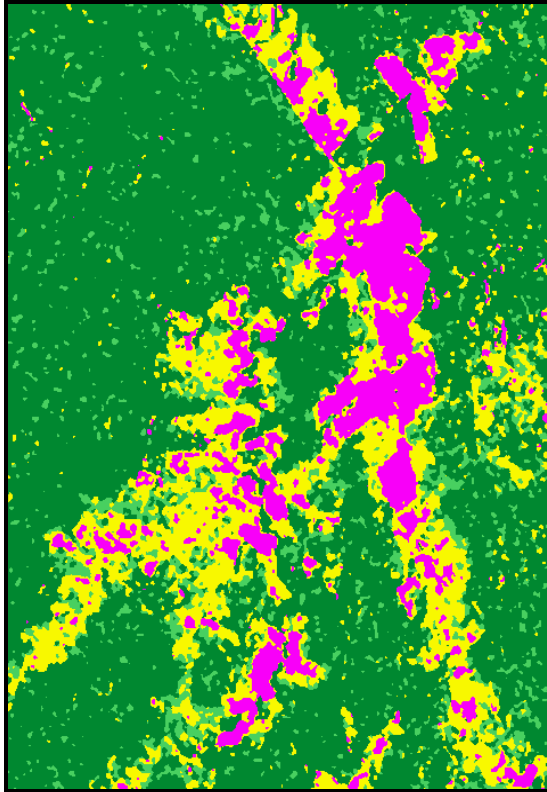


Figure 4: ICM classification using Sirc5 set.

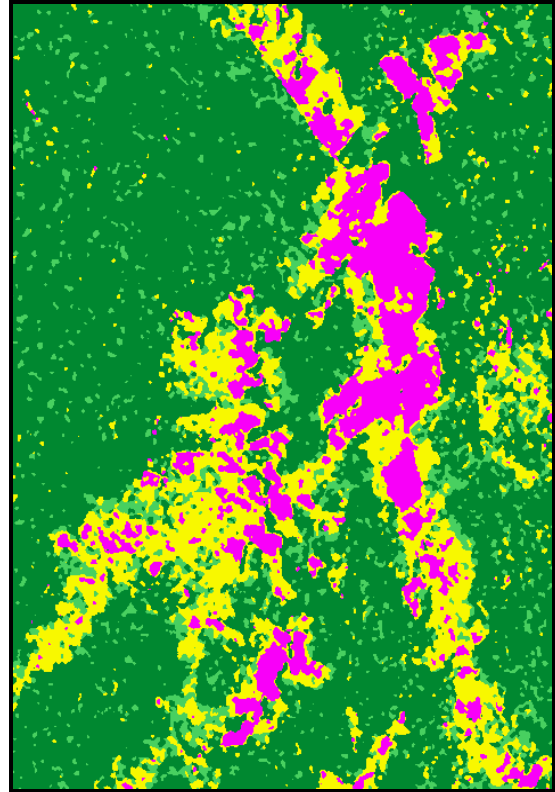


Figure 5: ICM classification using Sirc7 set.

TABLE 7 – Confusion matrix for the Sirc5 set classification.

Classes\ Classif	RecAct	NewReg	OldReg	Forest
RecAct	89.5	10.5	0.0	0.0
NewReg	7.1	50.7	19.5	22.7
OldReg	4.7	28.1	53.2	14.0
Forest	0.7	4.9	8.3	86.1
$\hat{K} = 0.4952$		$\hat{S}_K^2 = 2.3988 \times 10^{-5}$		

TABLE 8 – Confusion matrix for the Sirc7 set classification.

Classes\ Classif	RecAct	NewReg	OldReg	Forest
RecAct	89.5	10.5	0.0	0.0
NewReg	7.0	52.7	18.3	22.0
OldReg	5.5	28.5	53.9	12.1
Forest	0.6	5.1	8.7	85.6
$\hat{K} = 0.4967$		$\hat{S}_K^2 = 2.3355 \times 10^{-5}$		

The classification results obtained using Sirc4 and Sirc5 sets (**Figures 3 and 4**) were used to compare the discriminatory power carried by textural and tonal information. It can be noticed that the classification of the RecAct class is about the same (see **Tables 6 and 7**) when both types of information are used. The textural information contained in the selected features was important to improve the classification results of the Forest class. The results of classification using only features bands, presented in **Table 7**, show a significant decrease (close to 44%) of the OldReg pixels that were misclassified as NewReg class and a improvement (about 32%) of the pixels that were correctly classified as OldReg class. However, the misclassification of the OldReg pixels as Forest pixels increased when only features bands were used.

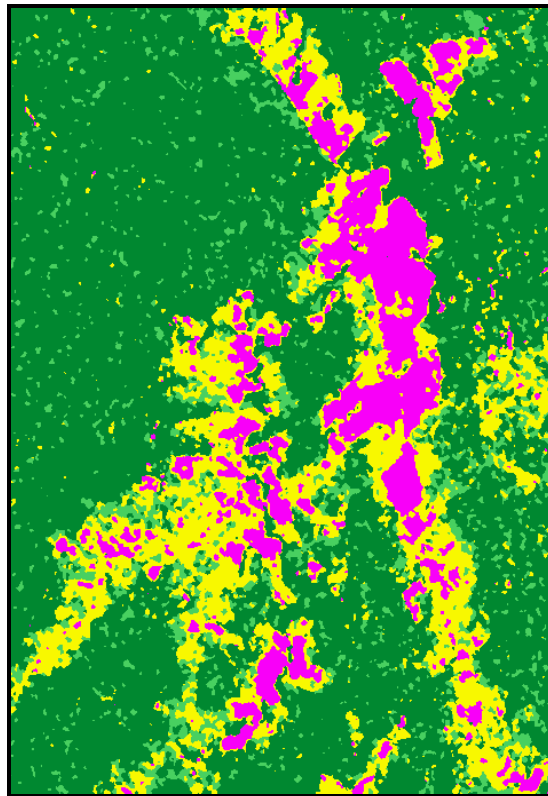


Figure 6: ICM classification using Sirc9 set.

TABLE 9 – Confusion matrix for the Sirc9 set classification.

Classes\ Classif	RecAct	NewReg	OldReg	Forest
RecAct	89.3	10.6	0.0	0.1
NewReg	7.0	56.8	18.0	18.2
OldReg	5.5	29.1	58.4	7.0
Forest	0.5	4.2	8.7	86.6
$\hat{k} = 0.5328$		$\hat{S}_K^2 = 2.2755 \times 10^{-5}$		

The classification results obtained for Sirc5 and Sirc7 sets (**Tables 7 and 8**) are very similar, meaning that the addition of the original L bands to the feature bands (Sirc5) did not improve the classification. This can be justified by the fact that $m_A(lhv)$ and $m_l(lhv)$ are included in the Sirc5 set, and they are features that gather tonal information. The result of z test gives no evidence to reject the hypothesis that the two Kappa values are different, at a confidence level of 95%. It might indicate that the tonal information carried by L-HH band/polarization has no influence on the classification results.

When comparing the results from the sets that use only L bands (Sirc2 and Sirc5), the classification results for Sirc5 are better than those obtained for Sirc2, which means that the features information discriminate better than only tonal information.

However, associating the textural information and the tonal information provided by four original bands (Sirc9 set) increase the percentage of pixels of the NewReg and OldReg classes that were correctly classified (**Table 9**), by decreasing the misclassification of pixels from these classes as belonging to the Forest class.

It can be seen from the classification results of the five sets that there is not a significant modification on the classification of the RecAct class. The use of the features bands or C bands on the classification decreases the misclassification of Forest pixels as regeneration classes, but the features bands seem to be better than C bands for this purpose. The Sirc5, Sirc7 and Sirc9 classifications (**Figures 4 to 6**) appear cleaner than those that only use the original bands (**Figures 2 and 3**). The areas of OldReg were better classified when the textural features and C bands are used.

The pixels of OldReg class misclassified as NewReg class is the largest error found on the classifications. It is of about 50% for Sirc2 and Sirc4 images and it is reduced by half for Sirc5, Sirc7 and Sirc9 images.

Using only the original bands (Sirc2 and Sirc4 sets) the RecAct was the class with the best classification (90% of the pixels), followed by Forest (66%), NewReg (64%) and OldReg (31%). When textural features are added, these percentages values are RecAct (89%), Forest (86%), OldReg (55%) and NewReg (53%). These results can be seen as good due to the complexity of the study area and taking into account that the classification was done using only radar images.

The z tests for all pairs of Kappa values were performed and they can be considered different at 95% confidence level, except for Sirc5 and Sirc7 sets. Therefore, the best classification result was obtained using Sirc9 set.

5 Conclusions

This work showed a methodology for analysis and selection of attributes (features) for image classification. The methodology was applied to SIR-C images aiming at the discrimination of four types of land use on the Brazilian Amazonia. From the results it can be concluded that the SIR-C images have good discriminatory potential to separate the classes of interest. The results presented in this paper encourages further studies in this field of research.

From the five selected features it could be noted that the L band has, in general, more information than the C band to discriminate the classes used in this study. The L-HV

band/polarization seems to be the best data to discriminate these classes. The selected features include textural and tonal information features showing that the both information are important for SAR image classification purposes. The α parameter of the K-Amplitude distribution shows gather some important textural information for discriminating regeneration classes from the others.

The best results were obtained for the classes of Recent Activities and Primary Forest, showing that is possible to map recent deforested areas using SIR-C data. The worst results of classification were obtained for New Regeneration and Old Regeneration. The task of discriminating these two classes is difficult even when using optical data (LANDSAT/TM images, for instance). The results showed that the Recent Activities class can be discriminated from the other classes using only tonal information, but textural attributes are necessary to discriminate the other classes. The C bands are important to discriminate Old Regeneration and Primary Forest classes. The use of features improves the classification of the Old Regeneration class by decreasing the misclassification of pixels from this class as New Regeneration class, but the confusion between these two classes are still large.

The distance measure used (Euclidean distance) to select the features with highest discriminatory power does not consider variations among and within classes. Thus other measures for selecting features may be used to improve the results. Other textural attributes (not only statistical and distributional) or another classification technique may be used to improve the classification results.

References

- Brown, S.; Lugo, A.. Tropical secondary forest. *Journal of Tropical Ecology*, 6, pp.1-32, 1990.
- Frery, A.C.; Müller, H.J.; Yanasse, C.C.F.; Anna, S.J.S A model for extremely heterogeneous clutter. *IEEE Trans. Geosc. Rem. Sens.*, 35(3):1-12, 1997a.
- Frery, A.C.; Yanasse, C.C.F.; Vieira, P.R.; Sant' Anna, S.J.S.; Rennó, C.D. A user-friendly system for synthetic aperture radar image classification based on grayscale distributional properties and context. Simpósio Brasileiro de Computação Gráfica e Processamento de Imagens, 10., 1997, p. 211-218. *SIBGRAPI 97*. Los Alamitos, CA, IEEE Computer Society, 1997b.
- Instituto Nacional de Pesquisas Espaciais (INPE). INPE atualiza os dados do desflorestamento na Amazônia, de 1995 a 1997. INPE Notícias, N° 13, p. 1-2, jan-fev de 1998.
- Le Toan, T.; Beaudoin, A.; Riou, J.; Guyon, D. Relating forest biomass to SAR data. *IEEE Trans. Geosc. Rem. Sens.*, 30:403-411, 1992.
- Luckman, A.J.; Frery, A.C.; Yanasse, C.C.F.; Groom, G.B. Texture in airborne SAR imagery of tropical forest and its relationship to forest regeneration stage. *International Journal of Remote Sensing*, 18 (6): 1333-1349, 1997a.
- Luckman, A.J.; Baker, J.; Kuplich, T.M.; Yanasse, C.C.F.; Frery, A.C. A study of the relationship between radar backscatter and regenerating tropical forest biomass for spaceborne SAR instruments. *Remote Sensing of Environment*, 60: 1-13, 1997b.

- Ma Z. and Redmond, R.L. Tau coefficients for accuracy assessment of classification of remote sensing data. *Photogrammetric Engineering and Remote Sensing*, 61(4):435-439, April, 1995.
- Ranson, K.J.; Saatchi, S.; Sun, G. Boreal forest ecosystem characterization with SIR-C/XSAR. *IEEE Transactions on Geoscience and Remote Sensing*, 33 (4): 867-876, July, 1995
- Schimel, D.; Enting, I.G.; Heimann, M.; Wigley, T.M.L.; Raynaud, D.; Alves, D.; Siegenthaler, U. CO₂ and the carbon cycle. In: Climate Change 1994, Radiative Forcing of Climate Change and An Evaluation of the IPCC IS92 Emission Scenarios. Cambridge University Press, pp.35-71, 1995.
- Sant'Anna, S.J.S.; Yanasse, C.C.F.; Hernandez, P.F.; Kuplich, T.M.; Dutra, L.V.; Frery, A.C.; Santos, P.P. Secondary forest age mapping in Amazonia using multi-temporal Landsat/TM imagery. In: 1995 International Geoscience and Remote Sensing Symposium, Italy, Jul. 10-14, 1995. *Quantitative remote sensing and applications*. Florence, Italy, IEEE, v. 1, p.323-325.
- Sant'Anna, S.J.S.; Yanasse, C.C.F.; Frery, A.C. Estudo comparativo de alguns classificadores utilizando-se imagens RADARSAT da região de Tapajós. In: Primeras Jornadas Latinoamericanas de Percepción Remota por Radar: Técnicas de Procesamiento de Imágenes. Buenos Aires, Argentina, dez.~1996, *Workshop Proceedings*. ESA, 1997, p. 187-194. (ESA SP-407).
- Soares, J.V.; Rennó, C.D.; Formaggio, A.R.; Yanasse, C.C.F.; Frery, A.C. An investigation of selection of texture features for crop discrimination using SAR image. *Remote Sensing of Environment*, 59 (2): 234-247, 1997.
- Vieira, P.R. *Desenvolvimento de classificadores de máxima verossimilhança e ICM para imagens SAR*. (MSc in Remote Sensing) – Instituto Nacional de Pesquisas Espaciais. São José dos Campos, SP, Brazil, 1996. 251 p. (INPE-6124-TDI/585).
- Vieira, P.R.; Yanasse, C.C.F.; Frery, A.C.; Sant' Anna, S.J.S. Um sistema de análise e classificação estatística para imagens SAR. In: Primeras Jornadas Latinoamericanas de Percepción Remota por Radar, Buenos Aires, Dez. 1996. *Técnicas de Processamiento de Imágenes*. Paris, ESA, 1997. p. 170-185.
- Yanasse, C.C.F.; Sant' Anna, S.J.S.; Frery, A.C.; Rennó, C.D.; Soares, J.V.; Luckman, A.J. Exploratory study of the relationship between tropical forest regeneration stages and SIR-C L and C data. *Remote Sensing of Environment*, 59 (2): 180-190, 1997.